Dynamic-Circulating-Current-Minimization Control for Isolated Three-phase AC-DC Converter with Matrix Converter

Hiroki Watanabe
Dept. of Electrical Electronics and Information Engineering
Nagaoka University of Technology
Nagaoka, Japan
hwatanabe@vos.nagaokaut.ac.jp

Jun-ichi Itoh
Dept. of Electrical Electronics and Information Engineering
Nagaoka University of Technology
Nagaoka, Japan
itoh@vos.nagaokaut.ac.jp

***Abstract*—This paper proposes a circulating current minimization control for an isolated AC-DC converter which combines a Dual Active Bridge (DAB) converter and a three-phase to single-phase matrix converter. The isolated AC-DC converter achieves Zero-Voltage-Switching (ZVS) to reduce switching losses. However, the circulating current occurs depending on the matrix converter`s transformer voltage and switching patterns. This paper proposes the Dynamic-Circulating-Current-Minimization (DCCM) control based on online calculation. The proposed control reduces the inductor RMS current with the wide operating region for the isolated three-phase AC-DC converter with the matrix converter. The experiment confirms the validity of the proposed control. The experimental results demonstrate that the transformer RMS current is reduced by 47% with the proposed DCCM control.**

Keywords—DAB converter, Matrix converter, Isolated AC/DC converter

I. INTRODUCTION

Electric Vehicles (EVs) are one of the major trends for future automotive applications owing to their non-carbon dioxide emission. Recently, EV chargers have been widely placed at fast-charging stations, parking lots, and housings to offer battery charging for EVs. The EV charger require some capability, e.g., (1) wide DC voltage control for battery charging, (2) galvanic isolation for human safety, and (3) high power density and a long lifetime to realize the high convenience for consumers [1]-[10].

The EV charger typically consists of a three-phase PWM rectifier and a bidirectional isolated DC-DC converter. This configuration assures the stable operation of the isolated three-phase AC-DC converter owing to the simple structure. Furthermore, the bidirectional isolated DC-DC converter has capable of galvanic isolation with the high-frequency transformer. Hence, the size of the isolation transformer is reduced compared to the low-frequency transformer. However, this circuit configuration requires some bulky passive components, such as the grid-tied inductor and the electrolytic capacitor. These components may become the cause of the increase in the circuit volume. Significantly, the electrolytic capacitor may decay the reliability of the EV charges due to its temperature dependence of the lifetime.

The isolated three-phase AC-DC converters applying a matrix converter have been actively researched [11]-[20]. The matrix converter directly converts the three-phase AC voltage to the high-frequency square voltage with several kilo Hz instead of the three-phase PWM rectifier. The attractive advantages of this converter are that the bulky grid-tied inductor and the electrolytic capacitor are not necessary. Moreover, the matrix converter combines with the DAB converter as the square waveform inverter to reduce the number of the conversion stage compared to the conventional two-stage configuration. The bidirectional power control realizes by the phase-shift modulation like the typical DAB converter. Furthermore, Zero-Voltage-Switching (ZVS) is achieved to reduce switching losses. According to these features, high power density and high conversion efficiency are expected by the isolated three-phase AC-DC converter with the matrix converter. The reduction of circulating current in the isolated three-phase AC-DC converter is important to improve conversion efficiency. The circulating current occurs depending on the condition of the transformer voltage and the switching patterns of the matrix converter. However, it is difficult to find the minimum condition of the circulating current because the matrix converter has complicated switching patterns.

This paper proposes the Dynamic-Circulating-Current Minimization (DCCM) control for the isolated three-phase AC-DC converter with the matrix converter. The new contribution of the proposed method is that the duty ratio is adjusted to minimize the circulating current according to the envelope of the input three-phase voltage. Besides, it is automatically optimized by online calculation in order to keep the minimum circulating current condition. According to the experimental result, the inductor current was reduced by 47% by the proposed control compared with the conventional method.

II. CIRCUIT CONFIGURATION AND OPERATION PRINCIPLE

Fig.1 shows the circuit configuration of the isolated three-phase AC-DC converter applying the matrix converter. The matrix converter converts the three-phase AC voltage to the high-frequency square voltage of more than several kilo Hz. The high-frequency transformer is placed between the matrix converter and the H-bridge converter for galvanic isolation. The phase shift modulation realizes the bidirectional power control to make the phase difference between the primary and secondary transformer voltage.

Fig. 2 shows the transformer voltage waveforms and the transformer current in the isolated three-phase AC-DC

converter. The peak value of the transformer primary voltage v_p is determined by the line voltage of the three-phase grid. The phase difference δ is given to decide the transmission power, the same as the DAB converter.

The transformer voltage conditions of v_p and v_s give the transformer current. The transformer current at each voltage condition is expressed as

$$i_1 = \frac{v_1 T_{sw}}{2L} D_a \tag{1}$$

$$i_2 = i_1 + \frac{(v_1 - NV_{dc}) T_{sw}}{2L} D_1 \tag{2}$$

$$i_3 = i_2 - \frac{(v_2 - NV_{dc}) T_{sw}}{2L} D_2 \tag{3}$$

$$i_4 = i_3 - \frac{NV_{dc} T_{sw}}{2L} D_b \tag{4}$$

where N is the turn ratio of the high-frequency transformer, V_{dc} is the DC voltage, L is the inductance, D_a, D_1, D_2, and D_b are the duty of each voltage condition, respectively.

Fig.3 shows the space vector diagram of the matrix converter [21]. The current command vector I_{in}^* is obtained by the current vector of I_{mid} and I_{min}. The relationship between each current vector is expressed as

$$I_{in}^* = I_{mid} + I_{min} \tag{5}$$

$$I_{mid} = \frac{i_1}{2} D_a + \frac{i_1 + i_2}{2} D_1 \tag{6}$$

$$I_{min} = \frac{i_2 + i_3}{2} D_2 \tag{7}.$$

According to these equations, the duty conditions are obtained as

$$d_a = a \sqrt{\frac{NV_{dc} i_{mid} v_{ratio\_a}}{P\left(1 + v_{ratio\_a}(a+1) + v_{ratio\_b} K\right)^2}} \tag{8}$$

$$d_1 = \sqrt{\frac{NV_{dc} i_{mid} v_{ratio\_a}}{P\left(1 + v_{ratio\_a}(a+1) + v_{ratio\_b} K\right)^2}} \tag{9}$$

$$d_2 = K d_1 \tag{10}$$

$$K = -k_1 \pm \sqrt{k_1^2 + 4k_2} \tag{11}$$

$$k_1 = \frac{(a+1) - v_{ratio\_a}}{v_{ratio\_b} - v_{ratio\_a}} \tag{12}$$

$$k_2 = \frac{i_{min}}{i_{mid}} \left(\frac{(a+1)^2 - v_{ratio\_a}}{v_{ratio\_b} - v_{ratio\_a}} \right) \tag{13}$$

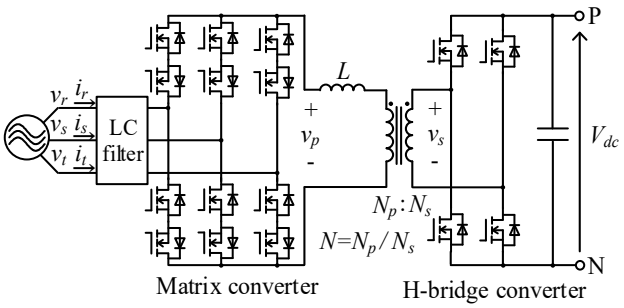

Fig.1. Isolated three-phase AC-DC converter with matrix converter.

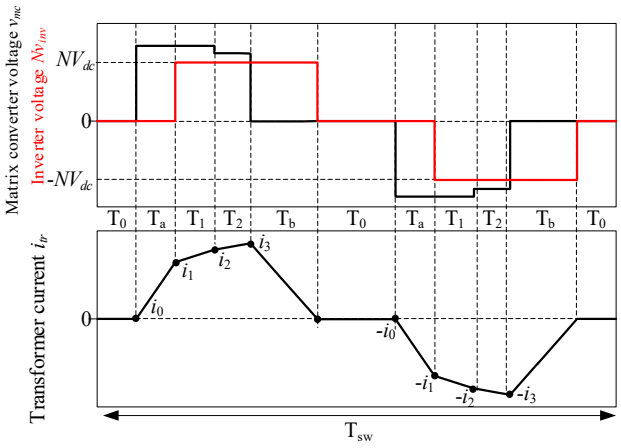

Fig.2. Each transformer voltage waveforms and transformer current in a high-frequency transformer.

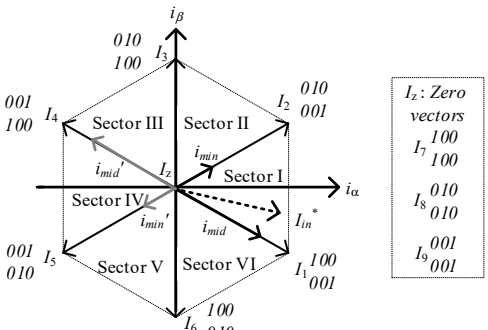

Ex.) I_1 100 Srp,Spr = ON, Ssp,Sps = OFF, Stp,Spt = OFF
001 Srn,Snr = OFF, Ssn,Sns = OFF, Stn,Snt = ON
※The number of "1" means switch is turn on.

Fig.3. Space vector diagram of matrix converter.

$$d_b = \frac{(a+1-v_{ratio\_a}) d_1 + (v_{ratio\_b} - v_{ratio\_a}) d_2}{v_{ratio\_a}} \tag{14}$$

$$d_0 = \frac{1 - ((a+1) d_1 + d_2 + d_b)}{2} \tag{15}$$

$$i_{ratio} = \frac{i_{min}}{i_{mid}} \tag{16}$$

$$v_{ratio\_a} = \frac{NV_{dc}}{v_{max}} \tag{17}$$

$$v_{ratio\_b} = \frac{v_{mid}}{v_{\max}} \tag{18}$$

where a is the ratio of d_a and d_1, and it is expressed as

$$a = \frac{d_a}{d_1} \tag{19}.$$

Note that a is the arbitrary constant. However, this parameter is very important in deciding the performance of the isolated three-phase AC-DC converter because the circulating current and the transmission power depending on the parameter of a. In the next chapter, the detail of the proposed control is introduced.

III. Dynamic-Circulating-Current-Minimization (DCCM) control

Fig.4 shows the relationship between the operation region and current mode in the isolated three-phase AC-DC converter. The operation region is separated by the current mode of the Continuous Current Mode (CCM) and the Discontinuous Current Mode (DCM). The green line means the boundary condition of each current mode. According to Fig.5, the circulating current occurs during the zero-voltage period of d_a and d_b because the current path to the power source does not make during this period. From (19), d_a depends on the ratio a. Hence, the parameter a influences the circulating current. The proposed DCCM control adjusts the parameter a to reduce the circulating current.

Fig.5 shows the flow chart of the calculation of a to minimize the circulating current. The parameter of a is calculated for each operating region of regions B, C, and D. The detail of the calculation is following.

A. Minimum circulating current condition in region B

Fig. 6 (a) shows the transformer voltage and transformer current waveforms in region B. The transformer current increases during d_a. On the other hand, the transformer current decreases during d_1 and d_2 due to the transformer voltage condition. Therefore, the proposed DCCM control adjusts the parameter of a to remove the period d_b. The parameter a in region B is derived from (8) to (15) when d_b equals zero, and it is expressed as

$$a = -1 + \frac{-r \pm \sqrt{r^2 - 4s}}{2} \tag{20}$$

$$\because r = -\frac{2v_{ratio\_a}}{1 + i_{ratio}\left(v_{ratio\_b} - v_{ratio\_a}\right)}$$

$$\because s = v_{ratio\_a}\frac{(1+i_{ratio})v_{ratio\_a} - i_{ratio}v_{ratio\_b}}{1 + i_{ratio}\left(v_{ratio\_b} - v_{ratio\_a}\right)}$$

B. Minimum circulating current condition in region C

Fig. 6 (b) shows the transformer voltage and transformer current waveforms in region C. In this region, d_a is set to zero because the transformer current increases during d_1 and d_2. Therefore, the proposed DCCM control adjusts the parameter of a to remove the period of d_a.

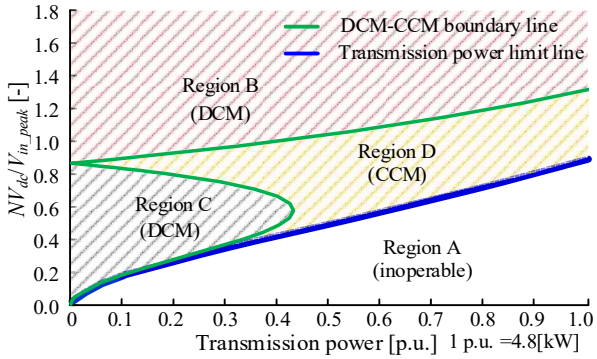

Fig.4. Relationship between the operating region and current mode in isolated three-phase AC-DC converter.

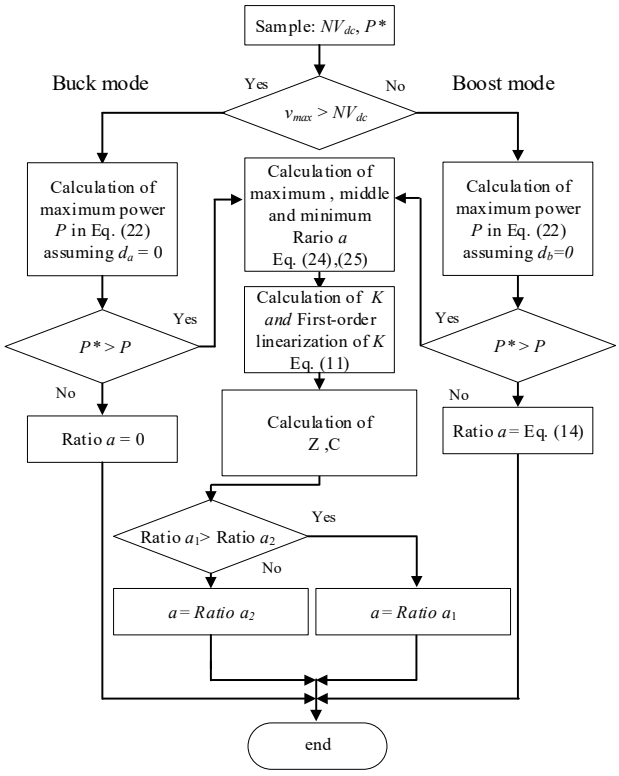

Fig.5. Flowchart of proposed DCCM control.

C. Minimum circulating current condition in region D

Fig. 6 (c) shows the transformer voltage and transformer current in region D. In this region, d_0 becomes zero because the transformer current is CCM without a zero-current period. In this region, it is necessary to calculate the non-linear equation to derive a. In order to derive the parameter a, the function K approximates the first-order equation as

$$K = Za + C \tag{21}$$

where Z is the coefficient of the first-order equation, and C is the intercept of the first-order equation. Note that K has two different slopes by the parameter a. Therefore, the approximated K is calculated by the polygonal approximation.

Firstly, the transmission power in region D is expressed as

$$P=\frac{NV_{dc}^{\ 2}}{4Lf_{sw}}\frac{(a+1)^2-v_{ratio\_a}}{\left(a\left(1+v_{ratio\_a}\right)+Kv_{ratio\_b}\right)^2} \tag{22}$$

where P is the transmission power, and f_{sw} is the switching frequency. The parameter a in region D is derived from (21) and (22), and it is expressed as

$$a=-b_1+\sqrt{b_1^2-c_1} \tag{23}$$

$$\because b_1=\frac{\left(1+v_{ratio\_a}+v_{ratio\_b}Z\right)\left(1+v_{ratio\_b}C\right)-\frac{NV_{dc}^{\ 2}}{4Lf_{sw}P}}{\left(1+v_{ratio\_a}+v_{ratio\_b}Z\right)^2-\frac{NV_{dc}^{\ 2}}{4Lf_{sw}P}}$$

$$\because c_1=\frac{\left(1+v_{ratio\_b}C\right)^2-\frac{NV_{dc}^{\ 2}+v_{ratio\_a}NV_{dc}^{\ 2}}{4Lf_{sw}P}}{\left(1+v_{ratio\_a}+v_{ratio\_b}Z\right)^2-\frac{NV_{dc}^{\ 2}}{4Lf_{sw}P}}$$

According to (22), the transmission power in region D depends on the parameter a. The parameter a with the maximum transmission power is obtained by the derivation of (22), and it is expressed as

$$a_{max}=v_{ratio\_a}\frac{2v_{ratio\_a}+\sqrt{2\left\{1+v_{ratio\_a}^{\ 3}\right\}}}{1+v_{ratio\_a}\left\{1-v_{ratio\_a}\right\}} \tag{24}.$$

According to (11) and (18), the function of K_{max} with the maximum transmission power in region D is obtained.

Next, the breaking point of the function K_b is calculated. The parameter a at the breaking point is calculated by the twice-derivation of (11), and it is expressed as

$$a_p=\frac{\sqrt{x_1+x_2+x_3x_4}-\{x_4+x_5\}}{x_4} \tag{25}.$$

$$\because x_1=i_{ratio}^{\ 2}\left\{v_{ratio\_a}^{\ 3}+v_{ratio\_a}^{\ 2}v_{ratio\_b}-2v_{ratio\_a}^{\ 2}v_{ratio\_b}\right\}$$

$$\because x_2=i_{ratio}\left\{v_{ratio\_a}^{\ 3}-v_{ratio\_a}^{\ 2}+v_{ratio\_a}v_{ratio\_b}-v_{ratio\_a}^{\ 2}v_{ratio\_b}\right\}$$

$$\because x_3=\left\{i_{ratio}v_{ratio\_a}(1+i_{ratio}(v_{ratio\_b}-v_{ratio\_a})-v_{ratio\_a})\right\}^{\frac{2}{3}}$$

$$\because x_4=1+i_{ratio}(v_{ratio\_b}-v_{ratio\_a})$$

$$\because x_5=v_{ratio\_a}$$

According to (11) and (25), the function of K_b at the breaking point is obtained.

Finally, the minimum value of K_{zero} is obtained when the parameter a is zero. The approximated line for the function of K_{zero} is obtained from the above three points of K_{max}, K_b, and K_{zero}. The parameter Z and C in (21) are obtained from the following equation

$$\{Z_{max-p},\ C_{max-p}\}=\left\{\frac{K_{max}-K_p}{a_{max}-a_p},\ \frac{K_pa_{max}-K_{max}a_p}{a_{max}-a_p}\right\} \tag{26}$$

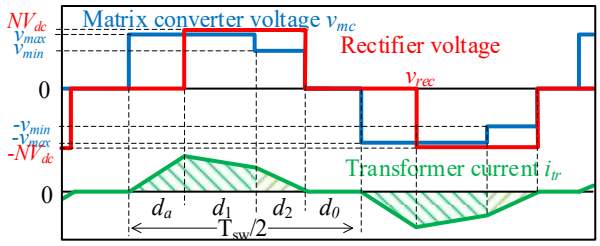

(a) Transformer voltage and current waveform in region B under DCM.

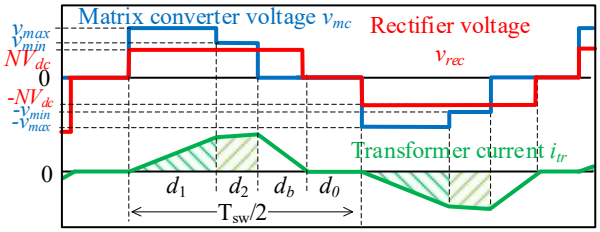

(b) Transformer voltage and current waveform in region C under DCM.

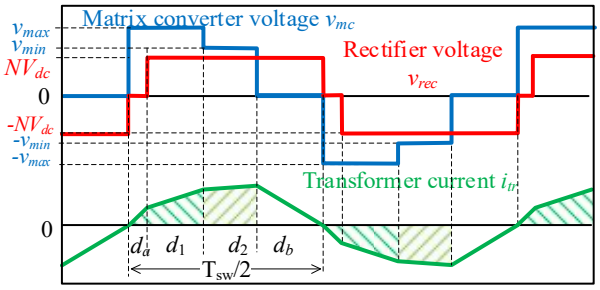

(c) Transformer voltage and current waveform in region D under CCM.

Fig.6. Transformer voltage and transformer current waveforms with different current mode.

$$\{Z_{p-0},\ C_{p-0}\}=\left\{\frac{K_p-K_0}{a_p},\ K_0\right\} \tag{27}$$

Fig.7 shows the control block diagram of the proposed DCCM control. the proposed control consists of a duty calculation, calculation of parameter a for minimization of the circulating current, and the switching pulse generator. The phase information is provided by the Phase Looked Loop (PLL). The switching duty is calculated by the phase current command, line voltage, DC voltage, and parameter a.

IV. Experimental Result

The validity of the proposed DCCM control is demonstrated by the experiment. Table I shows the experimental parameters. The grid voltage is 200 V_{rms}, the switching frequency is 50 kHz, and the rated power of the proto type circuit is 3.7kW. The DC voltage is set from 26V to 62V for buck and boost mode operation.

Fig.8 shows the U-phase current and the transformer current. According to Fig.8, the sinusoidal waveform of the U-phase current is obtained by the proposed DCCM control. The proposed DCCM control adjusts the control parameter of a in each operating region. The proposed DCCM control kept the low harmonic distortion for the grid current when the operation region was changed, as shown in Fig.8.

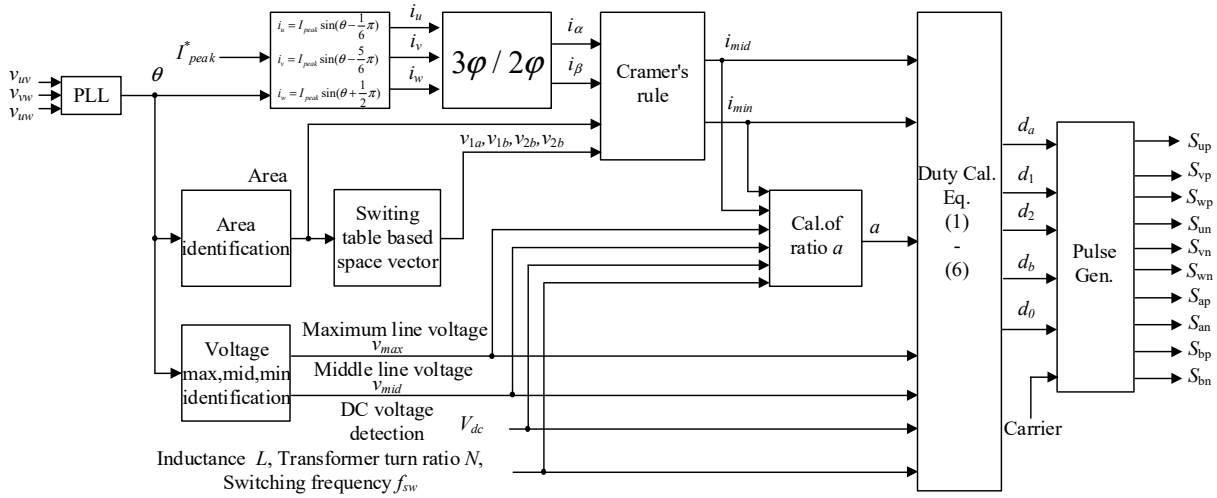

Fig.7. Control block diagram of proposed DCCM control.

Fig. 9 shows the transformer voltage and the transformer current when the operating condition is DCM and boost mode. According to Fig.9, the peak current of the transformer current is 36.0 A, and the transformer RMS current is 15.2A_{rms}. On the other hand, the proposed DCCM control reduces the transformer RMS current to 12.1A_{rms} from 15.2A_{rms} in the conventional control. In this condition, the transformer RMS current is reduced by 22.2%.

Fig. 10 shows the transformer voltage and the transformer current when the operating condition is DCM and buck mode. According to Fig. 10, the peak current of the transformer current is reduced when the proposed DCCM control is applied. In this condition, the transformer RMS current in the proposed DCCM control is reduced by 17.2% compared to that the conventional control.

Fig. 11 shows the transformer voltage and the transformer current when the operating condition is CCM and buck mode. According to Fig. 11, the peak current of the transformer current is reduced by 30.7% compared to the conventional method.

According to these experimental results, it was confirmed that the transformer rms current is reduced wide operating region by the proposed DCCM control. In the conventional control, the high transformer RMS current occurs due to the large circulating current. On the other hand, the proposed DCCM control reduces the circulating current in the transformer current. Therefore, the proposed control reduces the conduction losses and the copper loss in the isolated three-phase AC-DC converter.

Fig. 12 shows the transient test result when the transmission power is changed from 0.2 p.u. to 0.8 p.u.. In this condition, the operation mode is changed to CCM from DCM. Moreover, Fig. 12 (a) shows the test result when the operating region is changed to region D from region B. On the other hand, the Fig.12 (b) shows the transient test result when the operating region is changed to region D from region B. According to Fig.12, the operation mode is smoothly changed without current overshoots in Fig. 12 (a) and Fig. 12 (b).

Fig.13 shows the transformer current comparison with the conventional control and the proposed DCCM control. Note that the transformer current is compared at each operating region, as shown in Fig.4. According to Fig.13, it was confirmed that the transformer RMS current was reduced at all transmission power condition. Especially, the transformer current is reduced in all operating regions.

Table 1. Experimental parameter.

Quantity	Symbol	Value
Rated power	P	3.7 kW
Three-phase AC voltage	v_{ac}	200 V
DC voltage	V_{dc}	26~62V
Input frequency	f	50 Hz
Carrier frequency	f_{sw}	50 kHz
Leakage inductance	L	21.5 μH(%Z = 0.01 %)
Turn ratio of transformer	N_1:N_2	5.5:1
Input filter	L_f	0.19 μH (%Z = 1.0 %)
	C_f	10 μF (%Y = 5.0 %)
Dead-time	T_d	250 ns

V. CONCLUSIONS

This paper proposes the Dynamic-Circulating-Current Minimization (DCCM) control for the isolated three-phase AC-DC converter with the matrix converter. The new contribution of the proposed method is that the duty ratio is adjusted to minimize the circulating current according to the envelope of the input three-phase voltage. Besides, it is automatically optimized by the online calculation in order to keep the minimum circulating current condition. According to the experimental result, the inductor current in the proposed DCCM control was reduced by 47% compared with that of the conventional method.

REFERENCES

[1] E. Asa, O. C. Onar, V. P. Galigekere, G.-J. Su, B. Ozpineci, "A Novel Three-Phase Oak Ridge AC / DC Converter for Wireless EV Charger Applications" *IEEE Applied Power Electron. Conf. and Expo.*, pp. 437-443 (2021)

[2] M. Kwon, S. Choi "An Electrolytic Capacitorless Bidirectional EV Charger for V2G and V2H Applications" *IEEE Trans. on Power Electron.*,Vol. 32, No. 9 pp. 6792-6799 (2017)

[3] D. Mishra, B. S. Singh, B. K. Panigrahi,"Adaptive Current Control for a Bidirectional Interleaved EV Charger With Disturbance Rejection" *IEEE Trans. on Ind Appl.*,Vol. 57, No. 4 pp. 4080-4090 (2021)

[4] H. Kim, J. Park, S. Kim, R. M. Hakim, H. Belkamel, S. Choi,"A Single-Stage Electrolytic Capacitor-Less EV Charger With Single- and Three-Phase Compatibility" *IEEE Trans. on Power Electron.*,Vol. 37, No. 6 pp. 6780-6791 (2022)

[5] S. Dutta, S. Gangavarapu, A. K. Rathore, R. K. Singh, S. K. Mishra, V. Khadkikar,"Novel Single-Phase Cuk-Derived Bridgeless PFC Converter for On-Board EV Charger With Reduced Number of Components" *IEEE Trans. on Ind Appl.*,Vol. 58, No. 3 pp. 3999-4010 (2022)

[6] R. Kuchwaha, B. Singh, V. Khadkikar,"A Modified Luo Converter-Based Electric Vehicle Battery Charger With Power Quality Improvement" *IEEE Trans. on Trans Elect.*,Vol. 5, No. 4 pp. 1087-1096 (2019)

[7] J. Afsharian, D. Xu, B. Wu, B. Gong and Z. Yang, "The Optimal PWM Modulation and Commutation Scheme for a Three-Phase Isolated Buck Matrix-Type Rectifier," *IEEE Trans. on Power Electron*., vol. 33, no. 1, pp. 110-124 (2018)

[8] L. Zhou, M. Jahnes, M. Eull, W. Wang, M. Preindl,"Control Design of a 99% Efficiency Transformerless EV Charger Providing Standardized Grid Services" *IEEE Trans. on Power Electron.*,Vol. 37, No. 4 pp. 4022-4038 (2022)

[9] M. A. Sayed, K. Suzuki, T. Takeshita and W. Kitagawa: "Soft-Switching PWM Technique for Grid-Tie Isolated Bidirectional DC–AC Converter With SiC Device", *IEEE Trans. on Ind. Appl.* Vol. 53, No. 6, pp. 5602-5614 (2017)

[10] D. Das, N. Weise, K. Basu, R. Baranwal and N. Mohan: "A Bidirectional Soft-Switched DAB-Based Single-Stage Three-Phase AC–DC Converter for V2G Application", *IEEE Trans. on Transportation Electr.*, Vol. 5, No.1, pp.186-199 (2019)

[11] N. D. Weise, G. Castelino, K. Basu and N. Mohan: "A Single-Stage DualActive-Bridge-Based Soft Switched AC–DC Converter With Open-Loop Power Factor Correction and Other Advanced Features", *IEEE Trans. on Power Electron.*, Vol.29, No.8, pp. 4007-4016 (2014)

[12] J. Itoh, S. Nakamura, S. Takuma, H. Watanabe: "Isolated Three-phase AC to DC converter with Matrix Converter Applying Wide Output Voltage Operation", *2020 IEEE Energy Conv. Congr. and Expo.*, pp. 4563-4570 (2020)

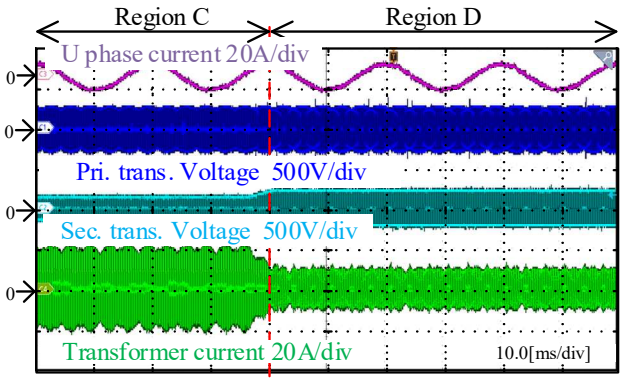

Fig.8. Experimental result of steady-state operation.

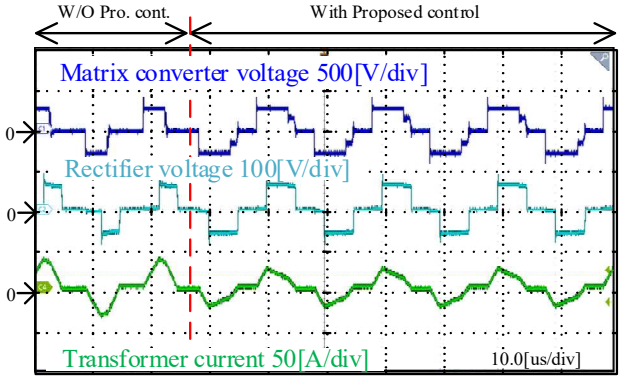

Fig.9. Transformer voltage and current in region B.

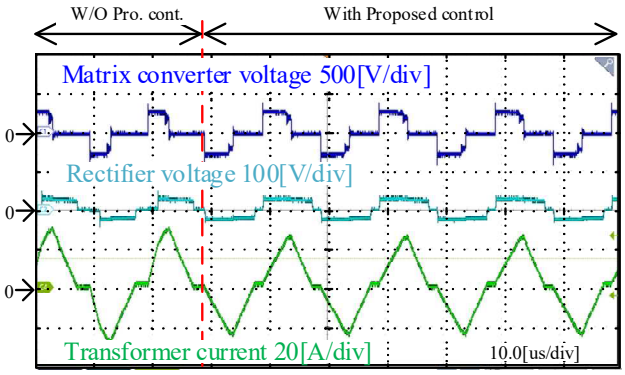

Fig.10. Transformer voltage and current in region.

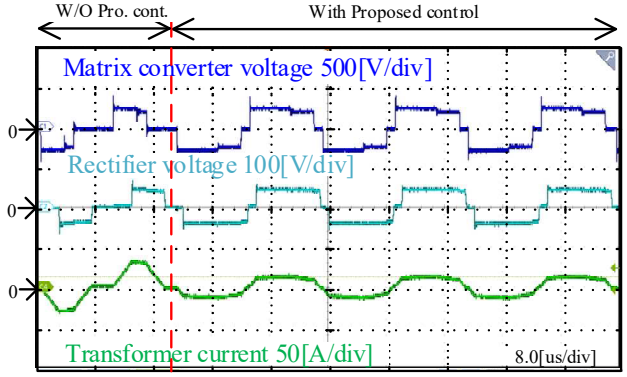

Fig.11. Transformer voltage and current in region D.

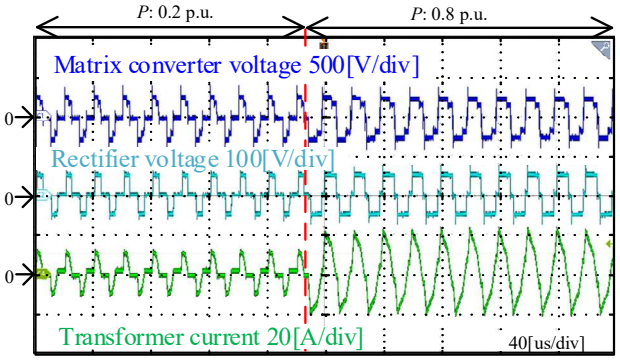

(a) Transient response from region B to region D.

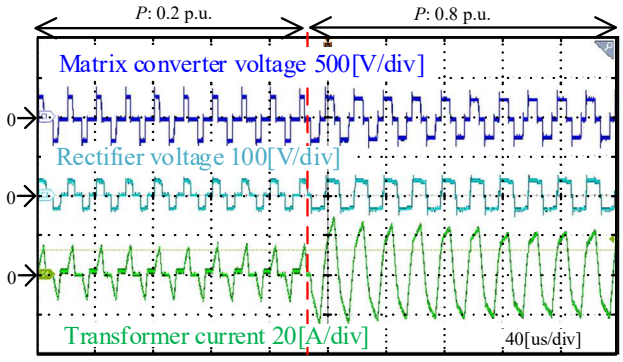

(b) Transient response from region C to region D.

Fig.12. Transient test result with proposed DCCM control.

[13] X. Z. Yue, L. Dongdong and S. S. Kumar, "An Optimal Modulation Technique and Duty Cycle Compensation in High Frequency Link Matrix Rectifier under DCM," *2019 IEEE 4th International Future Energy Electronics Conference (IFEEC)*, pp. 1-6 (2019)

[14] A. K. Singh, P. Das and S. K. Panda, "Novel switching scheme for matrix based isolated three phase AC to DC conversion," *IECON 2014* , pp. 3324-3329 (2014)

[15] T. Zhao, X. Guo, J. Su and D. Xu, "Improved space vector modulation for matrix converter based isolated rectifiers," *IECON 2014*, pp. 1532-1536 (2014)

[16] M. A. Sayed, K. Suzuki, T. Takeshita and W. Kitagawa, "Soft-Switching PWM Technique for Grid-Tie Isolated Bidirectional DC–AC Converter With SiC Device," *IEEE Trans. on Ind. Appl.*, vol. 53, no. 6, pp. 5602-5614 (2017)

[17] M. A. Sayed, T. Takeshita and W. Kitagawa, "Advanced PWM Switching Technique for Accurate Unity Power Factor of Bidirectional Three-Phase Grid-Tied DC–AC Converters," *IEEE Trans. on Ind. Appl.*, vol. 55, no. 6, pp. 7614-7627 (2019)

[18] L. Schrittwieser, M. Keibl, J. W. Kolar,"99% Efficiency Isolated Three-Phase Matrix-Type DAB Buck-Boost PFC Rectifier", *IEEE Trans. On Power Electron*, Vol. 35, no. 1, pp.138-157 (2020)

[19] K. Shigeuchi, J.Xu, N. Shimosato, Y. Sato, "A Modulation Method to Realize Sinusoidal Line Current for Bidirectional Isolated Three-Phase AC/DC Dual-Active-Bridge Converter Based on Matrix Converter", *IEEE Trans. On Power Electron*, Vol. 36, no. 5, pp.6015-6029 (2021)

[20] B. Feng, H. Lin, X. Wang, X. An and B. Liu, "Optimal zero-vector configuration for space vector modulated AC-DC matrix converter," *2012 IEEE Energy Conv. Congr. and Expo.*, pp. 291-297 (2012).

[21] S. Takuma, K. Kiri, H. Watanabe, J. Itoh: "Surge Voltage Reduction Method for DAB Matrix Converter using Circulating Current in Whole Load Condition", *2021 IEEE Energy Conv. Congr. and Expo.*, pp. 2301-2307 (2021)

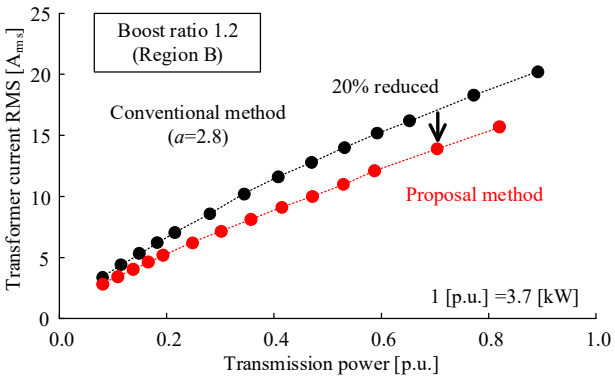

(a) Operation region B

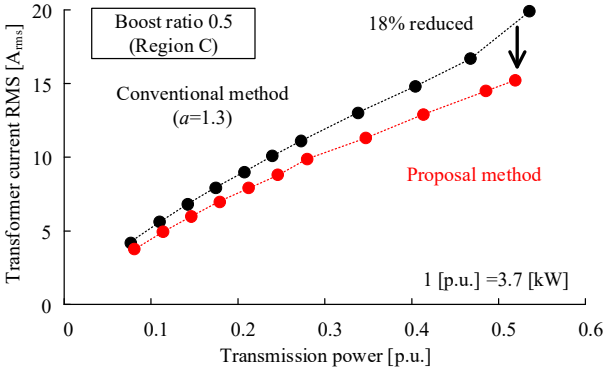

(b) Operation region C

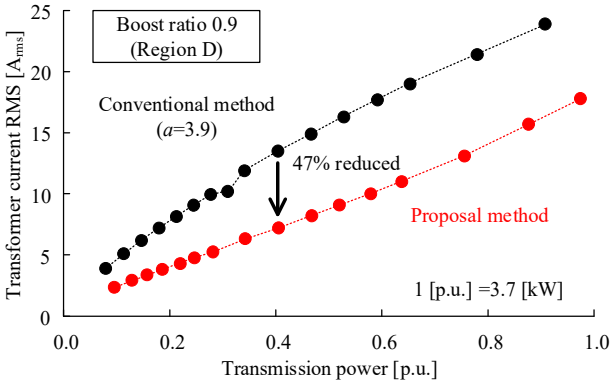

(c) Operation region D

Fig. 13. Transformer RMS current comparison results.